

# Vector chiral spin liquid phase in quasi-one-dimensional incommensurate helimagnets

Fabio Cinti,<sup>1,2,\*</sup> Alessandro Cuccoli,<sup>2</sup> and Angelo Rettori<sup>2</sup>

<sup>1</sup>*Department of Physics, University of Alberta, Edmonton, Alberta, Canada T6G 2J1*

<sup>2</sup>*Department of Physics, University of Florence and CNISM, 50019 Sesto Fiorentino (FI), Italy*

(Received 7 May 2010; revised manuscript received 28 February 2011; published 5 May 2011)

Making use of detailed classical Monte Carlo simulations, we study the critical properties of a two-dimensional planar spin model on a square lattice composed by weakly interacting helimagnetic chains. We find a large temperature window where the vector chirality order parameter,  $\langle \kappa_{jk} \rangle = \langle \mathbf{S}_j \times \mathbf{S}_k \rangle$ , the key quantity in multiferroic systems, takes nonzero value in the absence of long-range order or quasi-long-range order. The phase diagram we obtain for different strengths of the interchain coupling clearly shows that the weakness of the interchain interaction plays an essential role in order to observe the vector chiral spin liquid phase in a temperature range of up to now unattained width ( $\simeq 7\%$ , to be compared with  $\simeq 1\%$  or less previously reported for fully frustrated models, the only well-investigated systems unambiguously displaying spin-chirality decoupling). The relevance of our results for three-dimensional models is also discussed.

DOI: [10.1103/PhysRevB.83.174415](https://doi.org/10.1103/PhysRevB.83.174415)

PACS number(s): 64.60.De, 05.10.Ln, 11.30.Rd, 75.30.Kz

## I. INTRODUCTION

Geometrical frustration and/or competition between interactions can lead to exotic noncollinear magnetic thermodynamic phases, which can be characterized by unusual order parameters. Particularly relevant are two order parameters: scalar chirality,

$$\langle \chi_{jkl} \rangle = \langle \mathbf{S}_j \times \mathbf{S}_k \cdot \mathbf{S}_l \rangle, \quad (1)$$

and vector chirality, or spin current,

$$\langle \kappa_{jk} \rangle = \langle \mathbf{S}_j \times \mathbf{S}_k \rangle, \quad (2)$$

$j, k, l$  referring to neighboring sites of the lattice. These two chiralities present different symmetries: nonzero value of  $\langle \chi_{jkl} \rangle$  implies that the time-reversal symmetry is broken, while parity symmetry breaking comes when  $\langle \kappa_{jk} \rangle$  is different from zero.

Both of them are relevant in strongly correlated electron systems: Nonzero value of  $\langle \chi_{jkl} \rangle$  gives rise to the anomalous Hall effect<sup>1</sup> and leads to orbital electric currents in frustrated geometries,<sup>2</sup> while new phenomena emerge in Mott insulators as a consequence of induced scalar chirality, generated by the coupling between vector chirality and an external magnetic field.<sup>3</sup> On the other hand, relativistic spin-orbit interaction leads to a coupling between  $\langle \kappa_{jk} \rangle$  and the electric polarization<sup>4-7</sup> which play a fundamental role in magnetoelectric properties. This coupling also permits one to obtain experimental information about the vector chirality (which is difficult to measure owing to the absence of external fields that couple directly to  $\kappa_{jk}$ ): The chiral components in multiferroic  $\text{MnWO}_4$  have been detected by neutron diffraction using spherical polarization analysis as a function of temperature and of external electric field.<sup>8</sup>

Vector chirality, which is the argument of this paper, always accompanies helimagnetic (HM) order, and it can arise from spontaneous  $\mathbb{Z}_2$  symmetry breaking in systems with competitive exchange interactions,<sup>9</sup> or it can be stabilized by the Dzyaloshinskii-Moriya antisymmetric interaction in noncentrosymmetric compounds.<sup>6,10,11</sup> However, the chiral symmetry can anyway also be broken in a magnetically disordered state. Such a phase, where no magnetic order is

present but with  $\langle \kappa_{jk} \rangle \neq 0$ , is named a vector chiral spin liquid (VCSL) phase and has been intensively studied in previous years. It has been predicted to occur in one-dimensional ( $1d$ ) frustrated quantum magnetic systems<sup>12-14</sup> at zero temperature.

For higher dimension  $d$  it is crucial to understand if the VCSL phase is also stable in the presence of thermal fluctuations.<sup>14</sup> Indeed, having found a VCSL phase in a ( $1d$ ) quantum magnetic system, does not assure that such a phase is also present in a ( $2d$ ) classical magnetic system described by an apparently similar Hamiltonian. A given  $d$ -dimensional quantum model can indeed be mapped in a *suited* ( $d + 1$ )-classical model, but the latter is unknown unless an explicit mapping is available. For the system at hand a possible mapping was proposed by Kolezhuk,<sup>15</sup> who finally concluded for the appearance of a VCSL phase: a somewhat surprising conclusion, if one considers that the classical  $2d$  model obtained in Ref. 15 is the same already investigated by Garel and Doniach,<sup>16</sup> who did not find any VCSL. For  $d = 2$ , this phase has been clearly obtained at finite temperature  $T$  by classical Monte Carlo simulation (MCS) of a triangular lattice of spins with bilinear and biquadratic interactions<sup>17</sup> and for fully frustrated spin models.<sup>18</sup>

However, for models with longer range competing interactions leading to low-temperature incommensurate helimagnetic structures and  $d = 2, 3$ , a clear evidence of this exotic phase is yet lacking, even if Onoda and Nagaosa,<sup>19,20</sup> investigating a Ginzburg-Landau Hamiltonian describing helical magnets, suggest that a VCSL phase can be stabilized in  $d = 3$ . This prediction was questioned by Okubo and Kawamura:<sup>21</sup> Their classical MCS do not show any evidence of such a phase, but a first-order phase transition to a HM order.

It is important to note that in the quasi- $1d$   $XY$  organic magnet  $\text{Gd}(\text{hfac})_3\text{NITeT}$ <sup>22</sup> (a compound with high value of spin,  $S = 7/2$ ) a  $3d$  VCSL phase has been experimentally observed. This is due to the fact that  $d = 1$  is the lower critical dimension for an Ising order parameter, like  $\langle \kappa_{jk} \rangle$ , so that the chiral correlation length, which diverges exponentially at low  $T$ , is much larger than the spin correlation length, which diverges with a power law. Taking into account the interchain interaction within mean field approximation a  $3d$  VCSL phase

results at intermediate temperature.<sup>23</sup> However, theoretical results obtained considering also the interchain fluctuations are still lacking, and a direct numerical evidence of such a VCSL phase in quasi-1d system will be relevant.

In this paper we present the results obtained by employing accurate classical MCS to investigate a 2d spin system composed by weakly interacting helimagnetic chains. Despite the absence of apparent geometrical frustration (the model being defined on a square lattice), a clear separation in temperature between the chiral transition at  $T_c$  and the Kosterlitz-Thouless (KT) one to quasi-long-range order (QLRO) at  $T_{KT}$  can be observed, with  $T_c > T_{KT}$ . We will show that the weakness of the interchain interaction plays an essential role in order to get  $T_c > T_{KT}$  (i.e., to have the appearance of the VCSL phase).

The paper is organized as follows. In Sec. II we shall introduce the model Hamiltonian and subsequently both MCS techniques and the thermodynamic observable will be also discussed. In Sec. III the results will be presented. Finally, in Sec. IV, we shall discuss such results, also drawing some conclusions.

## II. MODEL HAMILTONIAN, MCS TECHNIQUES, AND THERMODYNAMIC OBSERVABLES

We consider a square lattice on the  $(x, y)$  plane composed of  $N = L \times L$  planar spins  $\vec{S}_{i,j}$  ( $|\vec{S}|=1$ ), with Hamiltonian:

$$\mathcal{H} = - \sum_{i=1}^L \sum_{j=1}^L \{ J_1 \vec{S}_{i,j} \cdot \vec{S}_{i,j+1} + J_2 \vec{S}_{i,j} \cdot \vec{S}_{i,j+2} + J' \vec{S}_{i,j} \cdot \vec{S}_{i+1,j} \}; \quad (3)$$

$j$  label spins along each chain, while  $i$  is the chain label. Intrachain exchange interactions are ruled by a nearest neighbor (NN), ferromagnetic (FM) coupling constant  $J_1$  and a next-nearest neighbor (NNN), antiferromagnetic (AFM) coupling  $J_2$ ; interchain NN spin interactions are ruled by the FM coupling constant  $J'$ . If the condition  $\delta \equiv |J_2|/J_1 > 1/4$  is fulfilled, the ground state corresponds to a HM order along the chains, with a pitch vector  $q_{\parallel} = \pm \cos^{-1}(1/4\delta)$ . In the following we take  $\delta = 0.3$ , i.e.,  $J_1 = 1$ , and  $|J_2| = 0.3$ , while  $T$  will be given in units  $J_1$ .

In order to build the phase diagram, the weakly interacting chain system has been investigated for  $J'$  ranging from  $0.05J_1$  to  $J_1$ ; detailed results will be shown mainly for  $J' = 0.1J_1$ , i.e., a representative value of the interchain coupling small enough to get the VCSL phase in a relevant temperature range, but not so small to require unusual care during the Monte Carlo simulation due to the presence of very different energy scales.

Periodic boundary conditions have been applied along the direction perpendicular to the chains, while free boundary conditions were taken along the chain direction, in order to avoid any undue bias interfering with possible incommensurate helix modulation.

Configuration sampling has been carried on making use of the usual Metropolis technique, while correlations between sampled configurations were mitigated by microcanonical over-relaxed moves.<sup>24</sup> For each simulated temperature at least three different runs have been performed, each run being composed of  $24 \times 10^6$  MC sweeps, with the first  $4 \times 10^6$

thermalization steps being discarded. Near the critical regions the multiple-histogram (MH) methods<sup>24</sup> were employed. Results for  $L = 24 - 128$  are reported.

Moving to the thermodynamic observables and their estimators, we start by introducing the order parameter related to the VCSL, the chirality, as

$$\kappa = \frac{1}{L(L-1) \sin q_{\parallel}} \sum_{ij} [\vec{S}_{ij} \times \vec{S}_{ij+1}]^z. \quad (4)$$

A suitable order parameter to test the helimagnetic order can be defined as

$$m_{\text{HM}} = K \int d q_{\parallel} S(\vec{q}), \quad (5)$$

where  $S(\vec{q})$  is the structure factor, with  $\vec{q} = (0, q_{\parallel})$ , and the normalization factor  $K$  is the reciprocal of the structure factor integral at zero temperature.<sup>25</sup> Both quantities defined in Eqs. (4) and (5) were calculated exclusively down the chain directions, where they are really relevant. In the investigation of the isotropic model considered by Garel and Doniach in Ref. 16, the following additional order parameter turns out to be especially useful:

$$M = \frac{1}{L} \sum_{i=1}^L m_i, \quad (6)$$

where

$$m_i = \sqrt{\left( \frac{1}{L} \sum_{j=1}^L S_{i,j}^x \right)^2 + \left( \frac{1}{L} \sum_{j=1}^L S_{i,j}^y \right)^2} \quad (7)$$

is the columnar magnetization perpendicular to the helical displacement. Indeed, as we will show in Sec. III, the quantity  $M$  defined in Eq. (6) turns out to be sensitive both for the VCSL and KT transitions.

In order to get more detailed, quantitative information about the critical regions under scrutiny (e.g., critical exponents and/or phase transition temperatures), we will also make use of quantities like the specific heat,

$$c_v = N\beta^2 (\langle e^2 \rangle - \langle e \rangle^2), \quad (8)$$

where  $\langle \dots \rangle$  denotes the thermodynamic average and  $e$  the energy per spin; the susceptibilities of the order parameters previously defined,

$$\chi_{\mathcal{O}} = N\beta (\langle \mathcal{O}^2 \rangle - \langle \mathcal{O} \rangle^2), \quad (9)$$

where  $\mathcal{O} = \kappa, m_{\text{HM}},$  and  $M$ ; and finally their Binder's fourth cumulants,<sup>24</sup>

$$u_4(\mathcal{O}) = 1 - \frac{\langle \mathcal{O}^4 \rangle}{3\langle \mathcal{O}^2 \rangle^2}. \quad (10)$$

Moreover, in order to investigate the *pure* KT transition, it is inevitable that the helicity modulus be introduced, too.<sup>26</sup> As it is well known, such an observable measures the response of the system to the application of a twist  $k_0$  on the boundary conditions,

$$\Upsilon(T) = \left. \frac{\partial^2 F(T)}{\partial k_0^2} \right|_{k_0=0}, \quad (11)$$

where  $F(T)$  is the free energy. In this paper, for obvious reasons, we choose  $k_0$  perpendicular to the chain directions, and we will look for the universal jump  $2/\pi$  of the quantity  $\Upsilon(T)/T$ , expected from scaling arguments as  $T \rightarrow T_{KT}$  in the thermodynamic limit  $L \rightarrow \infty$ .

### III. RESULTS

In Fig. 1 the specific heat *versus* the temperature is reported for three different cases:  $1d$  chain with  $\delta = 0.0$  (dashed line),  $1d$  chain with  $\delta = 0.3$  (continuum line), and the system described by the Hamiltonian (3) (symbols), respectively. The first two curves were obtained through the usual numerical transfer matrix technique.<sup>27,28</sup> For the nonfrustrated chain, we can easily recognize the usual broad maximum at  $T \sim 0.4$ . On the other hand, for  $\delta = 0.3$  a sharp maximum at  $T \sim 0.03$  is observed. Qualitatively, this sharp maximum can be attributed to the presence of chiral domain walls (solitons) in the helical short-range order phase, as extensively discussed by many authors in the last 20 years.<sup>29–31</sup>

The landscape becomes more challenging when the interchain interactions are turned on: For  $J' = 0.1J_1$ , in Fig. 1 we observe at  $T \simeq 0.12$  a well-defined narrow and sharp peak, having the typical shape we expect at a proper phase transition, so that we are led to relate it with the onset of the VCSL phase. The scaling behavior of  $c_v$  with  $L$  is reported in the inset of Fig. 1: We immediately observe as increasing  $L$  the peak more and more acquires the typical features associated with a second-order phase transition. Further increasing the temperature, a second broad and size-independent peak is observed at  $T \simeq 0.2$ , which is consistent with a KT scenario.

In order to estimate the critical temperatures, we employ the Binder's cumulant previously introduced in Eq. (10). The Binder cumulant for different  $L$  is reported in Figs. 2(a) and 2(b) for the chirality and the helical order parameters, respectively. For the chirality we can evaluate  $T_\kappa = 0.1176$  (6), while for the helical order parameter, we obtain  $T_{KT} = 0.1095$  (5). The data in Fig. 2 allow one to assert that the two critical

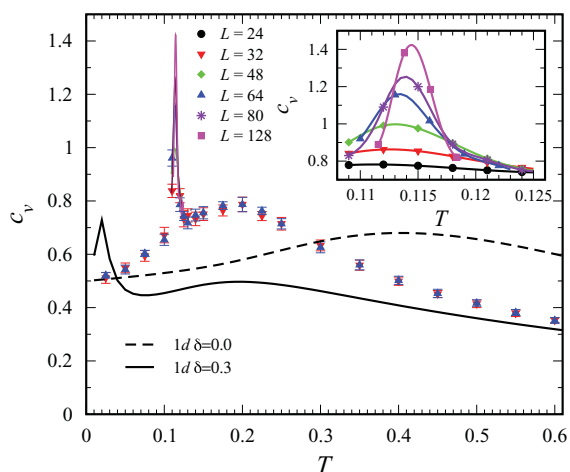


FIG. 1. (Color online) Specific heat versus temperature for the model (3) with  $J' = 0.1J_1$  for different  $L$  (see legend), and for  $1d$  model with  $\delta = 0.0$  and  $\delta = 0.3$ . (Inset) MH result (solid lines) around  $T_\kappa$  for different  $L$ .

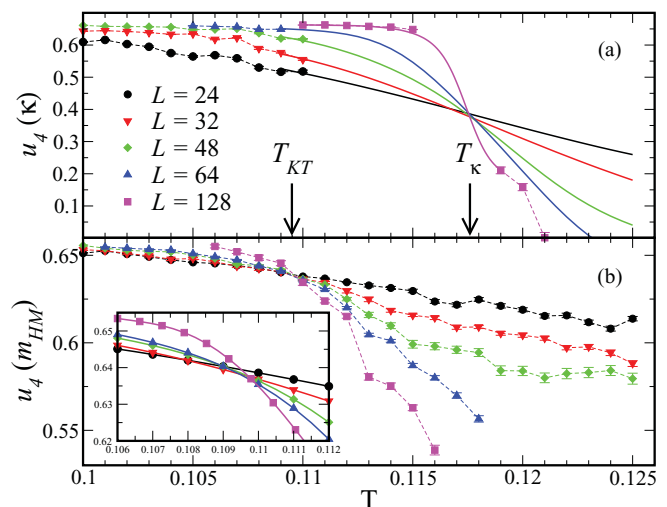


FIG. 2. (Color online) Binder cumulants versus temperature for different lattice sizes for the system with interchain interactions  $J' = 0.1J_1$  (solid lines, MH interpolation). (a)  $u_4$  for the order parameter  $\kappa$ . (b)  $u_4$  for the HM order parameter. (Inset) MH interpolation around  $T_{KT}$ .

temperatures are well distinguishable with  $(T_\kappa - T_{KT})/T_{KT} \simeq 7.4\%$ .

The identification of the crossing temperature in Fig. 2(b) as the KT transition temperature can be further validated by making use of the finite-size scaling (FSS) relation  $\chi_m(L) \propto L^{\gamma/\nu}$ ; a best-fit procedure gives  $\gamma/\nu = 1.77$  (3) (Fig. 3), fully consistent with the KT behavior of a  $2d$  planar system.

Another evidence of the presence of two distinct critical points comes from the scrutiny of the vortex density,<sup>32</sup>  $\rho$ . In the dilute-gas approximation, we have  $\rho \sim \exp(-2\mu/T)$ , where  $2\mu$  is the energy required to create a pair of vortices,<sup>33</sup> and it can be obtained by linear fit of  $-\ln \rho$  as a function of  $T^{-1}$ . From Fig. 4 three different regimes can be identified: low temperature ( $T < T_{KT}$ ), intermediate temperature ( $T_{KT} < T < T_\kappa$ ), and high temperature regime ( $T_\kappa < T$ ). The linear fit in the range  $T_{KT} < T < T_\kappa$  (solid line) gives an activation energy of dissociated vortex pairs greater than that obtained

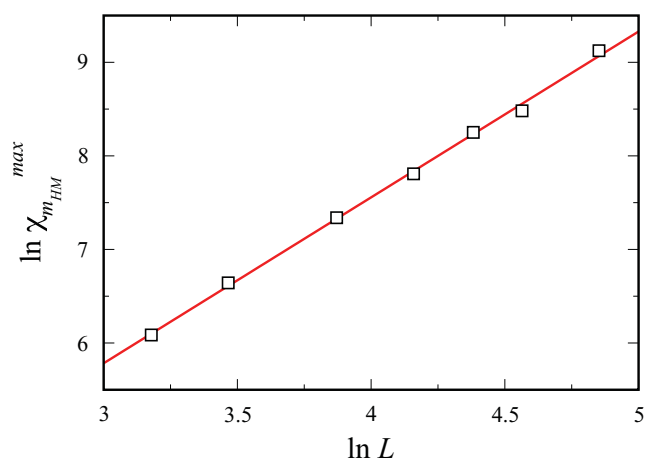


FIG. 3. (Color online) Logarithm of the maximum of  $\chi_{m, HM}$  as a function of  $\ln L$ . The error bars lie within the symbols (interchain interactions,  $J' = 0.1J_1$ ).

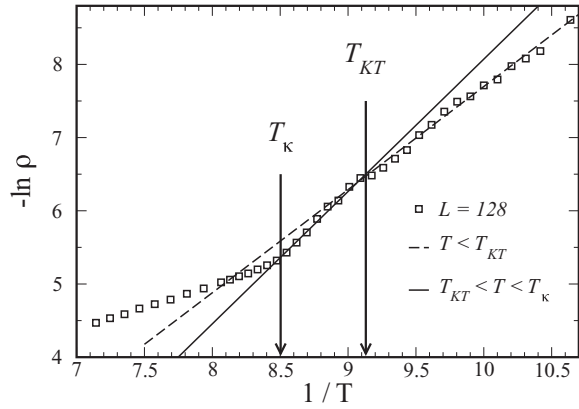


FIG. 4. Vortex density  $\rho$  versus  $T^{-1}$  for  $L = 128$  and  $J' = 0.1J_1$ , error bars lie within point size. (Continuum line) Linear regression in the SL region. (Dashed line) Linear regression in the KT regime.

for lower temperature  $T < T_{KT}$ , where all vortex pairs are bounded, with a clear slope change at  $T \simeq T_{KT}$ . Finally, the creation of other dissociated vortex pairs appears again easier in the region  $T > T_K$ , where  $\mu$  strongly decreases signaling the onset of a complete disorder; it is worth observing that the change of slope is located at  $T_K$  instead of at the maximum of the specific heat, and it is much more marked than in isotropic models displaying KT transitions.<sup>34</sup>

A proper characterization of the VCSL transition involves several aspects. A first central issue concerns the order of the transition. By analyzing the equilibrium energy distribution at  $T = T_K$ , no double-peaked structure is observed, even at the largest simulated size of the lattice  $L = 128$ . So we have no explicit indication for a first-order transition.

The universality class pertaining to the VCSL transition has been investigated by FSS analysis. In Fig. 5(a) the chiral susceptibility is displayed for different values of  $L$ . From the expected dependence of its peak position temperature on  $L$  [Fig. 5(b)], we can use the following relation,

$$T_K(L) = T_K + cL^{-\frac{1}{\nu}}. \quad (12)$$

Making use of the value of  $T_K$  previously obtained [Fig. 2(a)], we get the estimate  $\nu = 1.02$  (5) for the critical exponent  $\nu$ .

From the analysis of the peak values of  $\chi_K$  with the FSS relation  $\chi_K(L) \propto L^{\gamma/\nu}$ , we obtain the ratio  $\gamma/\nu = 1.66$  (7) [Fig. 4(c)], which implies  $\gamma = 1.70$  (8). These values of  $\gamma$  and  $\nu$  are in very fair agreement with  $\gamma = 7/4$  and  $\nu = 1$ , that is, the proper values of the Ising universality class in  $2d$ .

Concerning the critical exponent  $\alpha$  for the specific heat,<sup>35</sup> which for the Ising universality class in  $2d$  is 0, the  $c_v$ -peak values,  $c_v^{\max}(L)$ , versus  $L$  are very well fitted (see Fig. 6) by the FSS relation proper of the  $2d$  Ising model:

$$c_v^{\max}(L) = A + B \ln(L) + CL^{-1}. \quad (13)$$

The present exploration allows us to conclude that  $\alpha = 0$ , confirming unequivocally the Ising character of the VCSL transition.

We point out that the quasi-1d nature of the model is fundamental in order to obtain a VCSL phase, that is, chiral order in absence of QLRO. This has been explicitly checked in

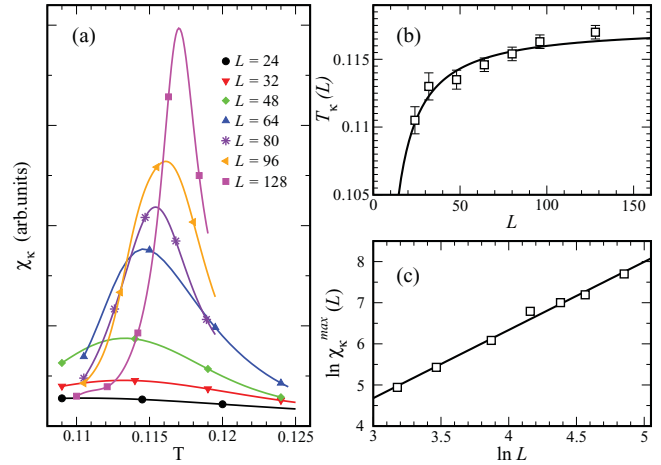


FIG. 5. (Color online) (a) Chiral susceptibility versus temperature by MH interpolation (solid lines) for different sizes. In (b) the temperature where the peak of  $\chi_K$  is located is reported versus  $L$ . In (c) the maximum value of  $\chi_K$  is reported as a function of  $\ln L$ . Error bars fall within the symbols (interchain interactions,  $J' = 0.1J_1$ ).

the range  $0.05 \leq J'/J_1 \leq 1$ . In Figs. 7(a)–7(d) a summary of the obtained results is reported for  $J' = J_1$ , that is, the model investigated by Garel and Doniach.<sup>16</sup>

For the specific heat in Fig. 7(a) we observe a size-independent broad peak at  $T \simeq 0.75$ , consistent with a KT scenario, while a size-dependent, narrow peak at  $T \simeq 0.34$  is found. Using the helicity modulus (11), we estimate  $T_{KT} \simeq 0.45$ . On the other hand, for the largest simulated size ( $L = 108$ ), the chiral susceptibility (9) shows a narrow peak at the same temperature  $T_K$  of the narrow, size-dependent, specific heat peak and, above all,  $T_K$  is significantly lower than  $T_{KT}$ . These data are corroborated by looking at the order parameter defined in Eq. (6). As the susceptibility associated with the parameter  $M$  results sensitive to both two- and four-point correlations, a first anomaly is observed at a higher temperature, which stabilizes at  $T_{KT}$  when  $L$  increases, signaling the onset of the quasicrystal; subsequently, at lower temperature,  $\chi_M$  has a second anomaly at a temperature

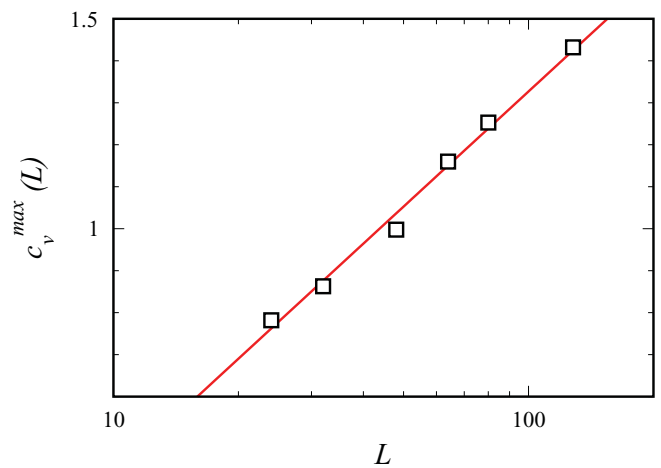


FIG. 6. (Color online) Maximum of the specific heat versus  $L$  (error bars lie within point size). Continuum line, fit function; see text.



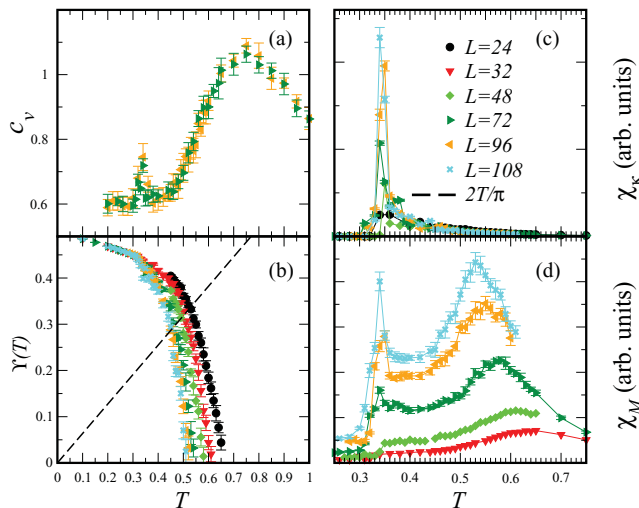


FIG. 7. (Color online) Observables calculated for the system with  $J_1 = J'$  for different size  $L$ : (a) specific heat; (b) helicity modulus; (c) chiral susceptibility; (d) susceptibility of  $M$  (see text).

consistent with those already displayed by the specific heat and the chiral susceptibility: We can thus definitely estimate  $T_\kappa \simeq 0.34$ . For  $J' = J_1$  a clear separation between the KT behavior and chiral setup is again present, but, at variance with the quasi-1d case, the onset of the chiral order is established at a temperature  $T_\kappa$  lower than  $T_{KT}$ ; the results of our MCS rule out completely the scenario proposed in Ref. 15 about the behavior of the investigated 2d classical model, and confirm the predictions of Ref. 16.

In Fig. 8(a) complete phase diagram of  $T_{KT}$  and  $T_\kappa$  versus the ratio  $J'/J_1$  is reported: Only when the interchain coupling is sufficiently weak,  $J'/J_1 \lesssim 0.1$ , the VCSL phase appears in a sensible range of temperature.

#### IV. DISCUSSION AND CONCLUSION

In conclusion, we have presented the outcomes of intensive MCS for a 2d XY classical spin system, defined on a square lattice, composed by weakly interacting frustrated chains. We observe a clear separation between the VCSL phase and the QLRO phase only when  $J' \lesssim 0.1J_1$ , where  $T_\kappa > T_{KT}$ . The onset of the VCSL phase displays the typical features of a second-order phase transition, consistent with the 2d Ising universality class, and for this weakly coupled incommensurate helimagnet the chiral spin liquid phase turns out to persist in a temperature range much wider than that reported for fully frustrated models (see Fig. 8). This result confirms the intriguing possibility of an emergent finite-temperature phase showing chiral long-range order in the absence of the helical one as investigated by many authors in the multiferroic context.<sup>14,17,19,20</sup>

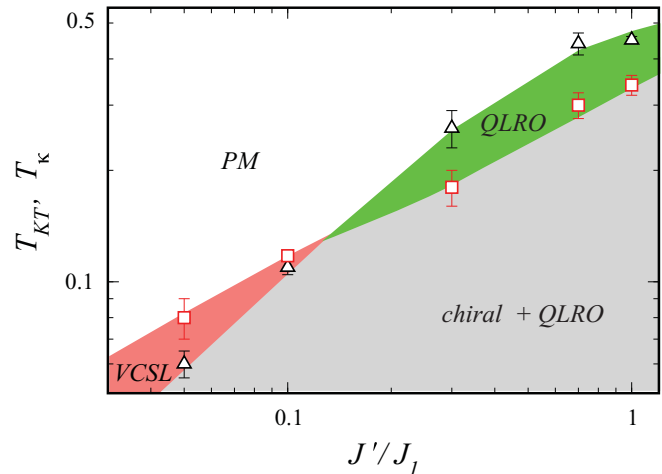


FIG. 8. (Color online) Phase diagram  $T_{KT}$  and  $T_\kappa$  versus interchain interaction strengths.

We found the quasi-1d nature of the system being crucial for observing this exotic phase: Indeed, assuming  $J' \lesssim J_1$  we find that the sequence of phase transitions can be reversed, that is,  $T_\kappa < T_{KT}$  (see again Fig. 8). When dealing with the existence of a 3d VCSL (the KT transition should now be replaced by a proper second-order one), we remind that for classical antiferromagnets on a 3d stacked-triangular lattice numerical simulations supported the occurrence of a single HM phase transition<sup>21</sup> even if in the 2d lattice  $T_\kappa > T_{KT}$  is observed.<sup>18</sup> However, we believe reasonable to hypothesize that for a 3d collection of weakly interacting HM chains the two transitions could remain well distinct, making it still possible to observe the VCSL phase. Such expectation follows from two motivations: (i) the surprising large temperature range where the VCSL phase is observed in 2d, for small values of  $J'/J_1$ ; (ii) at variance with the classical antiferromagnets on the 3d stacked-triangular lattice, where the interplane exchange interaction is at least comparable with the intraplane one, making it able to wash out the richness of the phase diagram observed in 2d, the weakness of the interchain interaction in our model should protect the sequence of the phase transitions observed for 2d even when moving to 3d. Further support to the outlined scenario emerged from the results of recent experiments on the quasi-1d organic high-spin magnet  $\text{Gd}(\text{hfac})_3\text{NITet}$ .<sup>22</sup>

#### ACKNOWLEDGMENTS

F.C. thanks INSTM, the Natural Science and Engineering Research Council of Canada under Research Grant No. 121210893, and the Alberta Informatics Circle of Research Excellence (iCore); financial support was also received from the Italian Ministry of University within the 2008 PRIN program (Contract No. 2008PARRTS\_003).

\*cinti@ualberta.ca

<sup>1</sup>Y. Machida, S. Nakatsuji, Y. Maeno, T. Tayama, T. Sakakibara, and S. Onoda, *Phys. Rev. Lett.* **98**, 057203 (2007).

<sup>2</sup>L. N. Bulaevskii, C. D. Batista, M. V. Mostovoy, and D. I. Khomskii, *Phys. Rev. B* **78**, 024402 (2008).

<sup>3</sup>K. A. Al Hassanieh, C. D. Batista, G. Ortiz, and L. N. Bulaevskii, *Phys. Rev. Lett.* **103**, 216402 (2009).

- <sup>4</sup>H. Katsura, N. Nagaosa, and A. V. Balatsky, *Phys. Rev. Lett.* **95**, 057205 (2005).
- <sup>5</sup>M. Mostovoy, *Phys. Rev. Lett.* **96**, 067601 (2006).
- <sup>6</sup>I. A. Sergienko and E. Dagotto, *Phys. Rev. B* **73**, 094434 (2006).
- <sup>7</sup>S. Cheong and M. Mostovoy, *Nat. Mater.* **6**, 13 (2007).
- <sup>8</sup>T. Finger, D. Senff, K. Schmalzl, W. Schmidt, L. Regnault, P. Becker, L. Bohaty, and M. Braden, *J. Phys.: Conf. Ser.* **211**, 012001 (2010).
- <sup>9</sup>H. Kawamura, *J. Phys. Condens. Matter* **10**, 4707 (1998).
- <sup>10</sup>C. Pfeleiderer, S. R. Julian, and G. G. Lonzarich, *Nature (London)* **414**, 427 (2001).
- <sup>11</sup>P. Pedrazzini, H. Wilhelm, D. Jaccard, T. Jarlborg, M. Schmidt, M. Hanfland, L. Akselrud, H. Q. Yuan, U. Schwarz, Y. Grin *et al.*, *Phys. Rev. Lett.* **98**, 047204 (2007).
- <sup>12</sup>T. Hikihara, L. Kecke, T. Momoi, and A. Furusaki, *Phys. Rev. B* **78**, 144404 (2008).
- <sup>13</sup>J. Sudan, A. Lüscher, and A. M. Läuchli, *Phys. Rev. B* **80**, 140402 (2009).
- <sup>14</sup>S. Furukawa, M. Sato, and S. Onoda, *Phys. Rev. Lett.* **105**, 257205 (2010).
- <sup>15</sup>A. K. Kolezhuk, *Phys. Rev. B* **62**, R6057 (2000).
- <sup>16</sup>T. Garel and S. Doniach, *J. Phys. C: Sol. St. Phys.* **13**, L887 (1980).
- <sup>17</sup>J.-H. Park, S. Onoda, N. Nagaosa, and J. H. Han, *Phys. Rev. Lett.* **101**, 167202 (2008).
- <sup>18</sup>M. Hasenbusch, A. Pelissetto, and E. Vicari, *J. Stat. Mech.: Theory and Experiment* (2005) P12002.
- <sup>19</sup>S. Onoda and N. Nagaosa, *Phys. Rev. Lett.* **99**, 027206 (2007).
- <sup>20</sup>N. Nagaosa, *J. Phys. Condens. Matter* **20**, 434207 (2008).
- <sup>21</sup>T. Okubo and H. Kawamura, *Phys. Rev. B* **82**, 014404 (2010).
- <sup>22</sup>F. Cinti, A. Rettori, M. G. Pini, M. Mariani, E. Micotti, A. Lascialfari, N. Papinutto, A. Amato, A. Caneschi, D. Gatteschi *et al.*, *Phys. Rev. Lett.* **100**, 057203 (2008).
- <sup>23</sup>J. Villain, *Ann. Isr. Phys. Soc.* **2**, 565 (1978).
- <sup>24</sup>D. Landau and K. Binder, *A Guide to Monte Carlo Simulations in Statistical Physics* (Cambridge University Press, Cambridge, 2005).
- <sup>25</sup>F. Cinti, A. Rettori, and A. Cuccoli, *Phys. Rev. B* **81**, 134415 (2010).
- <sup>26</sup>P. Chaikin and T. Lubensky, *Principles of Condensed Matter Physics* (Cambridge University Press, Cambridge, 2000).
- <sup>27</sup>R. Baxter, *Exactly Solved Models in Statistical Mechanics* (Academic Press, London, 1982).
- <sup>28</sup>J. Thijssen, *Computational Physics* (Cambridge University Press, Cambridge, 1999).
- <sup>29</sup>I. Harada, *J. Phys. Soc. Jpn.* **53**, 1643 (1984).
- <sup>30</sup>F. Bartolomé, J. Bartolomé, C. Benelli, A. Caneschi, D. Gatteschi, C. Paulsen, M. G. Pini, A. Rettori, R. Sessoli, and Y. Volokitin, *Phys. Rev. Lett.* **77**, 382 (1996).
- <sup>31</sup>M. Affronte, A. Caneschi, C. Cucci, D. Gatteschi, J. C. Lasjaunias, C. Paulsen, M. G. Pini, A. Rettori, and R. Sessoli, *Phys. Rev. B* **59**, 6282 (1999).
- <sup>32</sup>Because free boundary conditions along the chain were taken it is possible to observe the existence of unpaired vortex (antivortex). However, their contribution to the vortex density results absolutely negligible.
- <sup>33</sup>D. R. Nelson, *Phase Transition and Critical Phenomena*, Vol. 7 (Academic Press, New York, 1983) and references therein.
- <sup>34</sup>R. Gupta and C. F. Baillie, *Phys. Rev. B* **45**, 2883 (1992).
- <sup>35</sup>M. N. Barber, *Phase Transition and Critical Phenomena*, Vol. 8 (Academic Press, New York, 1983).